ingegneria sismica
International Journal of Earthquake Engineering
Anno XLIII - Num. 1 - 2026

Real-Time State Estimation and Security Early Warning of Distribution Networks under IoT Edge Computing Architecture

Yingjie Liang[1] *and Shuzhen Tan*[1,*]

[1] Guangxi Electrical Polytechnic Institute, Nanning 530299, Guangxi, China

SUMMARY: *The real-time state estimation and safety early warning are the two most important components of the distribution network management of power systems. The conventional strategies cannot satisfy the current grid requirements of efficiency, accuracy, and real-time response. In order to overcome this, this paper utilizes an edge computing-based multi-objective ant colony distributed algorithm to carry out distributed state estimation in distribution networks, which eliminates the computational time and accuracy constraints of conventional state estimation strategies. To ensure safety early warning a fault information matrix is defined to determine faulty sections. Faults on line segments are defined based on predefined threshold conditions, allowing thorough safety monitoring of the distribution network. The combination of the suggested models of state estimation and safety detection forms an IoT-based real-time state estimation and safety early warning system of distribution networks. It continuously estimates states, identifies faults, and sends safety warnings. In its application to check a three-feeder armored buried cable system in one facility, the system correctly determined that the first feeder was the faulty one, which is how it really was. It shows the promising potential of the system applications.*

KEYWORDS: *Edge Computing; Multi-Objective Ant Colony Optimization; State Estimation; Safety Early Warning; Distribution Network*

1 Introduction

In line with the dual carbon targets, there is a slow increase in the penetration rates of electric vehicles, distributed energy resources, energy storage units and various flexible loads in the distribution grids. It results in large-scale distributions, additional nodes and more complicated designs that convert conventional passive distribution networks with one-way power flows into active distribution networks with two-way power flows [1-4]. The irregular power delivery of distributed energy generation, together with the random charge and discharge processes of electric vehicles and energy storage devices can cause sudden variations in the condition of power distribution systems [5-7]. Due to the constant growth of distributed energy, electric vehicles and renewable energy, along with the ever-increasing number of consumers who are now active players in the electricity market, the smart evolution of distribution grids requires stricter requirements in terms of system operation and control. Such requirements introduce new issues to the safety and real time distribution grid monitoring [8-10]. Determination of the current operational status of the grid is one of the key tools of the state estimation and security alerting, which makes a significant contribution to the implementation of fault detection, grid reconfiguration, demand response and other advanced grid management services [11, 12]. They

*13317700342@163.com
https://doi.org/10.65102/is2026486
Published: 30 April, 2026

have become the fundamental elements to achieve reliability, performance, and safe operation of distribution networks.

The distribution system estimation (DSE) is a procedure where high-precision, complete, and reliable active state of a distribution network can be estimated using different measurement information, including distribution network measurement data, non-remotely sensed telemetry data, and busbar load forecast data, in combination with algorithms that are appropriate to the properties of the distribution network [13]. The current major technologies in DSE can be broadly grouped into two categories: Static Distribution System Estimation (DSSE) and Dynamic Distribution System Estimation (DDSE). The most developed state estimation algorithm used in distribution systems is Weighted Least Squares (WLS)-based DSSE. Ajoudani et al. have improved WLS by taking into consideration load changes during measurement periods, duration of data transmission, and time spent on calculating state variables. They also improved the smart meter variance to minimize the error in state variable estimation and increase active DSE accuracy [14]. Fault location in distribution networks with limited measurement information provided by distributed smart metering devices was addressed by Ling et al. using a state estimation algorithm based on WLS. They recognized faults by comparing detected values with fault branches, which were calculated and simulated on real-time basis [15].

The general algorithms used in DDSE are formulated in accordance with the Kalman Filter (KF) theory. Ferreira et al. developed a dynamic model of active distribution networks using KF as well as a static measurement model incorporating the dynamics of active equipment into the state dynamic equations. It changes the estimation procedure of DSE allowing estimating the state of distribution networks with low monitoring levels [16]. Researchers Kettner and Paolone have applied the sequential discrete KF to develop a DDSE estimator. The estimator works with synchronized phasor measurement conditions in phase measurement devices (PMUs) and has similar performance to discrete KF [17]. Taking into account the dynamics of active distribution networks with different PV output, Wu et al. came up with an interval DDSE that depends on the square-root-of-trace KF. The method uses neural networks to calculate PV output intervals and a normal fluctuation range model of active distribution networks, which allows tracking dynamic grid states [18]. Wang et al. dealt with nonlinearity and Gaussian distribution in distribution systems by combining Kopman operator theory with the Kalman particle filters. Through this method, it was possible to build a model-independent DDSE in distribution systems that improved the precision of DDSE when dealing with dynamic systems and noisy measurements at various conditions of Gaussian distribution [19]. While WLS can also be employed for DDSE evaluation tasks, research by Watitwa and Awodele indicates that for active DDSE processes, the extended KF method outperforms WLS-based approaches when the model is correctly constructed [20]. This is because KF is typically not an optimal estimator; filtering may diverge if initial state estimates are erroneous or process modeling is incorrect. Furthermore, the predictive model for KF state variables has limitations. KF functions correctly only when the state space model and noise statistics are known and accurate. Incorrect selection of filter types can also cause the algorithm to be sensitive to measurement errors and system scale [21, 22].

Hybrid State Estimation (DHSE) is a method that freely selects measurement data and combines state estimators, enabling differentiated choices of measurements and estimators based on the specific performance requirements and varying estimation time needs of advanced systems [23]. Huang et al. integrated real-time monitoring and data acquisition system data with metering infrastructure data, and combined data-driven estimators, topology identification, and model-based estimators. They implemented estimator switching under fluctuations in metering infrastructure data, thereby forming the DHSE method [24]. In distribution networks,

DRSE enables management systems to respond in real time to operational and emergency events, thereby supporting grid reliability and energy efficiency. Its fundamental applications include reactive power management, outage management, loss reduction, adaptive overcurrent protection, condition-based maintenance, and integration with transmission system operations [25-27]. The real-time state estimation (DRSE) is usually deployed based on DSSE, DDSE, or DHSE. Džafić and Jabr used the sequential WLS and power flow computation to create new scaling formulas of loads at loop nodes. They obtained radial and multiphase DRSE incorporating sensitivity-based methods of measuring voltage magnitude in radial distribution networks with estimation efficiency exceeding the traditional three-phase voltage equations [28]. In a similar fashion, Liu et al. utilized real-time smart meter information, taking voltage and load pseudo-measurement as state variables and real-time measurement compensation data, respectively. They were able to achieve DRSE of three-phase four-wire low-voltage distribution systems through WLS and a load estimation model that involves clustering and partial least squares regression, which also addressed the problems of real-time data storage and asymmetry [29]. Manousakis and Korres have created a new learning model using a neural network structure that was inspired by electric power grid models to decrease the amount of parameterized mappings in DRSE and improve model stability. This was then implemented along with a greedy algorithm to reduce the complexity of neural networks when placing PMUs to allow the use of existing measurement data of PMUs to perform DRSE [30]. Soltani and Khorsand combined polar-coordinate power-voltage and rectangular-coordinate current-voltage representations. Integrating micro-PMU and smart meter data, they observed measurements at each time interval to achieve DRSE and real-time topology detection [31]. Cavraro et al. employed asynchronous DRSE, processing data through iterative updates based on approximate point types. Their estimator supplements measurements retrieved within specific time windows, refining details during continuous data acquisition [32].

Compared to real-time state estimation in distribution networks, research on real-time safety early warning systems for distribution networks remains limited. Chen et al. constructed a probabilistic model considering the uncertainties of electric vehicles and renewable energy. They employed probabilistic power flow and dynamic sensitivity weighting analysis to calculate weights for multiple distribution network operational risk factors and conduct time-series-based evaluations. Integrating a conditional value-at-risk model and early warning criteria that account for economic risks, they determined risk levels and zones before visualizing risks to complete the early warning process [33]. GU et al. proposed an intelligent mining algorithm for operational fault early warning in distribution networks during extreme weather, leveraging data mining. By uncovering correlations between weather data and distribution network operational data, they enabled risk prediction and effective early warning for distribution network operations [34]. Highly penetrated distributed power sources impact distribution network load states. Gu et al. employed complex network theory to create dynamic models and voltage overvoltage risk indicators for distribution networks. With the help of the Monte Carlo methods to collect random power characteristics and sense the load state, they evaluated and computed risks, which allowed them to provide early warning and risk control depending on the results [35]. Low voltage distribution network operational risks load characteristic digital twin early warning model was proposed by Zho et al. This model has five steps: data acquisition -> load feature extraction -> early warning scope expansion -> adaptive monitoring deployment -> risk identification and tracking -> risk correction and handling [36]. The risk early warning model and real-time optimization model were built by Zhang et al. using distribution network operational data and imitation learning respectively. Having trained and optimized the risk early warning model using historical risk data, they combined the two models to allow real time risk evaluation and early detection using incomplete real time data [37]. Real-

time operational data, historical outage data, weather data and condition of the equipment were all integrated by Gan et al. Using Long Short-Term Memory (LSTM) networks and gradient-boosted trees, they estimated the status of the active distribution network, produced early warnings, and activated emergency response systems. Such a method had a warning accuracy of 92 percent and a false alarm rate of less than 3.6 percent [38]. An online monitoring and early warning system of ground fault arcing in distribution networks was created by Zhang et al. It is based on IoT, triple exponential smoothing and genetic algorithms to allow real-time data gathering and smart forecasting to provide visual early warnings [39].

Real-time status monitoring and safety alerting of power distribution networks cannot be done without the help of IoT devices. Nevertheless, due to the rapid increase in the number of IoT devices and the more pressing requirements with respect to real-time performance, low latency, and data privacy protection, the shortcomings of traditional centralized cloud computing architectures have been demonstrated over time [40, 41]. In such a context, edge computing has become a new paradigm of computing, providing new opportunities and solutions to the IoT architectures. As scholars Bablu and Rashid pointed out, edge computing can solve the problem of latency, bandwidth, privacy, and security when operating real-time data processing using IoT. Furthermore, through the synergy of technologies like artificial intelligence, 5G, and blockchain, it collectively innovates the IoT ecosystem [42]. Consequently, IoT edge computing architectures have become a crucial technical foundation for real-time state estimation and security early warning technologies in distribution networks. Since information and evaluation efficiency during DSE processes fluctuate with updates to local decision metrics, Pegoraro et al. reported changes in PMU measurement data to the DSE for estimation. By integrating measurement device data with a cloud-based IoT platform, they enabled the DSE to adaptively enhance accuracy under both local decision metrics and IoT modes [43]. He et al. employed IoT technology to construct a distribution network state risk early warning system. They determined detection indicators based on risk indicator weighting calculations, analyzed detected indicators, conducted risk assessments, and thereby determined distribution network states for early warning [44]. Huang et al. employed cloud-based model training and edge computing to monitor external conditions of distribution networks in real time and process data. With the assistance of machine learning algorithms and pattern recognition techniques, they analyzed and predicted the severity of external disruptions. This approach was integrated with a visualization system for real-time warning display and decision-making [45].

To address the computational speed and accuracy limitations of traditional state estimation methods, this paper first designs a distributed state estimation privacy computation approach centered on coordinated variables. Building upon conventional nonlinear state estimation models, an improved linear state estimation method is proposed to enhance computational efficiency. Subsequently, a multi-objective ant colony distributed solution algorithm for edge computing is introduced to implement the proposed distributed state estimation. For safety early warning in distribution networks, fault-related features are extracted. Based on these features, the detection device-branch correlation matrix and its element conditions are defined for the edge computing model. After acquiring and correcting fault information, a fault information matrix is constructed. Fault detection on line segments is performed based on the matrix elements, enabling safety monitoring of the distribution network. Integrating the proposed state estimation and safety detection models establishes an IoT-based real-time state estimation and safety early warning system for distribution networks. The system's practicality is validated through case studies.

2 Real-Time State Estimation Model for Distribution Networks Based on Edge Algorithms

The growth of distribution grids and the introduction of renewable energy and distributed power sources have made distribution grids larger in size and more complicated in topology, which are problematic to state estimation and safety early warning. The present study aims at providing solutions to these issues in form of real-time state estimation and safety detection algorithms of distribution grids using edge computing to create a real-time state estimation and safety early warning system on an IoT architecture.

The current chapter will be devoted to the state estimation of distribution networks. This is an application of a multi-objective ant colony distributed algorithm to edge computing to undertake distributed state estimation that can be used to overcome computational speed and accuracy constraints of conventional distribution network state estimation schemes.

2.1 Edge Algorithm Principles

2.1.1 Principles and Technical Architecture

Edge computing represents a distributed computing model that allocates computing capabilities among edge devices like substations and intelligent terminal devices in proximity to data generation sites, enabling on-the-spot data processing and instantaneous decision-making [46]. The technical design includes edge node devices such as precise sensors (like current transformers, temperature sensors), edge gateways incorporating FPGAs or ARM chips, and edge servers enabling containerization. The edge computing algorithms adopt light artificial intelligence models (for instance, pruned CNN, LSTM) or rule-based engines designed for resource-scarce environments to carry out data feature extraction and anomaly detection. In particular, the classification of equipment status can be achieved using the algorithm as shown in Equation (1):

$$y = \sigma\left(\sum_{i=1}^{n} w_i x_i + b\right) \tag{1}$$

Here, x_i represents sensor input features, w_i denotes model weights, o is the activation function, and the output y characterizes the probability of device anomalies. Communication Protocol allows for fast and dependable data exchange, including the 5G URLLC technology (Ultra-Reliable Low Latency Communication, with an air interface delay of less than 1 ms) used to communicate important control signals and LoRa, which is ideal for monitoring data from long distances with low power consumption. In edge computing, resource optimization must strike a balance between processing power and energy consumption. For instance, through task scheduling, resource allocation at the edge node can be optimized using linear programming, as shown in Equation (2):

$$\min \sum_{i=1}^{k} (E_i + \alpha T_i) \tag{2}$$

where E_i represents task energy consumption, T_i denotes processing time, and α indicates the weighting coefficient, ensuring high-priority tasks are executed first.

2.1.2 Degree of Compliance with Distribution Network Requirements

The technical features associated with edge computing match very well with those of distribution grids. The uniqueness of edge computing is seen in its ability to enable fault localization in the grid within milliseconds. This is facilitated by localized processing in edge nodes that bring down data round trip latencies from about hundreds of milliseconds in clouds to less than 10 milliseconds. Taking traveling wave fault location as an example, edge nodes directly analyze the time difference Δt between the wavefronts of traveling currents. Combined with the wave velocity v, this enables calculation of the fault distance, as shown in Equation (3):

$$d = v \cdot \Delta t / 2 \tag{3}$$

Addressing Latency Losses in Connection to Cloud Transmission. The design of the reliable architecture will allow the edge nodes to continue the transmission process even after network failures and to provide redundant storage on the side of the edge node, ensuring the basic monitoring functions even in the event of failure in connection. Data security and regulatory compliance. The data related to the operation of the distribution network is related to the users' personal data security and grid security. The edge computing system uses local encryption and data anonymization to not transmit raw data elsewhere.

2.2 Distributed State Estimation Model

2.2.1 Solving Nonlinear Models

Based on the distributed state estimation approach, the centralized state estimation is improved to the following model:

$$\begin{cases} Z_i(t) = S_i(t)X_i(t) + \xi_i(t) + \psi_i(t) \\ Z_e(t) = S_e(t)X_e(t) + \xi_e(t) + \psi_e(t) \end{cases} \tag{4}$$

In the formula, $Z_i(t)$ represents the intra-cluster measurement and state estimation model; $Z_e(t)$ represents the inter-cluster boundary coordination measurement and state estimation model.

$$\begin{cases} f(X(t)) = \min\{g(X_i(t)) + y(X_e(t))\} \\ g(X_i(t)) = \sum_{j=1}^{N_i}\{[Z_j(t) - S_j(t)X_j(t) - \psi_j(t)]^T \cdot \\ \qquad \Omega_j(t)[Z_j(t) - S_j(t)X_j(t) - \psi_j(t)]\} \\ y(X_e(t)) = \sum_{k=1}^{N_i}\{[Z_k(t) - S_k(t)X_k(t) - \psi_k(t)]^T \cdot \\ \qquad \Omega_k(t)[Z_k(t) - S_k(t)X_k(t) - \psi_k(t)]\} \end{cases} \tag{5}$$

In the equation, $g(X_i(t))$ denotes the state estimation function for nodes within the cluster; $y(X_e(t))$ denotes the state estimation function for boundary nodes of the cluster; N_1 represents the total number of clusters; N_2 represents the total number of boundary variables.

As seen from Equation (6), optimal state estimation ensures the minimum total estimation error across all clusters in the system, encompassing both internal and boundary nodes. Traditionally, the solution for estimating the state of any internal or boundary node is as follows:

$$\begin{cases} X(k+1) = X(k) + G^{-1}(k)\Pi^T \Omega[Z(t) - S(t)X(t) - \psi(t)] \\ \Pi = \partial[S(t)X(t)] / \partial X(t) \\ G(k) = \Pi^T \Omega \Pi \end{cases} \tag{6}$$

In the equation, Π denotes the Jacobian matrix, whose elements represent partial derivatives with respect to variable $X(t) = \dot{V}_b(t)$; G denotes the gain matrix; $k+1.k$ indicates the $k+1.k$ th iteration.

Equation (6) primarily employs a method involving matrix-based partial derivatives and iterative solution, which suffers from low computational efficiency and does not adopt a distributed solution approach. This paper proposes improvements to address these limitations.

2.2.2 Improved Rapid Linear Solving Model

The measurement includes the voltage phasors and current phasors measured at the node, as well as the current phasors on the transmission line. Therefore, the power flow equation on the transmission line can be expressed as the measurement equation:

$$\tilde{S}_{ij} = P_{ij} + jQ_{ij} = \dot{V}_i \left[\frac{\dot{V}_i - \dot{V}_j}{x_{ij}} \right]^* \tag{7}$$

In the equation, $\tilde{S}_{ij}$ represents the complex power on transmission line ij, with the two end nodes being i, j; P_{ij}, Q_{ij} denotes the active and reactive powers on transmission line ij, respectively; $\dot{V}_i, \dot{V}_j$ represents the voltage phasors at node i, j; x_i is the reactance on transmission line ij; the symbol * indicates conjugate. All quantities in equation (7) are normalized.

Dividing both sides of equation (7) by the voltage phasor $\dot{V}_i$ yields:

$$\frac{\tilde{S}_{ij}}{\dot{V}_i} = P_{ij} + jQ_{ij} = \left[\frac{\dot{V}_i - \dot{V}_j}{x_{ij}} \right]^* \tag{8}$$

At different measurement instants, due to minor variations in $\dot{V}_i$ and as a state estimate, let $\dot{V}_i^t$ denote the disturbance quantity over time. Consequently, fluctuations occur near the measurement of this quantity:

$$1 + \dot{V}_i^t = \dot{V}_i \tag{9}$$

In the equation, $1+\dot{V}_i$ represents the normalized voltage phasor of the reference node. Under normalized conditions, the voltage magnitude typically fluctuates around 1.

Substituting equation (9) into equation (10) yields:

$$\frac{\tilde{S}_{ij}}{1+\dot{V}_i^t} = P_{ij} + jQ_{ij} = \left[\frac{\dot{V}_i - \dot{V}_j}{x_{ij}}\right]^* \tag{10}$$

Perform a Taylor expansion of the constant $1/(1+\dot{V}_i^t)$ in equation (10) and use a linear approximation to obtain:

$$\begin{aligned}\frac{1}{1+\dot{V}_i^t} &= 1-\dot{V}_i^t + (\dot{V}_i^t)^2 - (\dot{V}_i^t)^3 + \cdots \\ &= \sum_{k=0}^{\infty}(-1)^n(\dot{V}_i^t)^n \approx 1-\dot{V}_i^t\end{aligned} \tag{11}$$

Neglecting the higher-order terms in equation (11) and retaining only the first two terms, combined with equation (9), yields:

$$\frac{1}{1+\dot{V}_i^t} \approx 1-\dot{V}_i^t = 1-(\dot{V}_i - 1) = 2-\dot{V}_i \tag{12}$$

Substituting equation (13) into equation (11) yields:

$$(2-\dot{V}_i)\tilde{S}_{ij} \approx P_{ij} + jQ_{ij} = \left[\frac{\dot{V}_i - \dot{V}_j}{x_{ij}}\right]^* \tag{13}$$

Similar to Equation (9), for measurements of quantities injected at node m—such as node voltage phasors and injected current phasors—the power flow equations can be expressed in terms of power:

$$\left[\tilde{S}_m\right]^* = P_m - \mathrm{j}Q_m = \dot{V}_m^* \sum_{i=1}^{n}(Y_{mi}\dot{V}_i) \tag{14}$$

In the equation, $[\tilde{S}_m]^*$ denotes the conjugate of the injected complex power at node m; P_m, Q_m represents the injected active and reactive powers at node m; $\dot{V}_m, \dot{V}_m^*$ denotes the voltage phasor and its conjugate at node m; n is the total number of nodes; Y_{mi} is the element in row m, column i of the system admittance matrix; $\dot{V}_i$ is the voltage phasor at node i.

Rewrite Equation (14) in the form of Equation (10) as:

$$P_m + jQ_m = \dot{V}_m \sum_{i=1}^{n}(Y_{mi}\dot{V}_i)^* \tag{15}$$

In the equation, $(Y_{mi}\dot{V}_i)^*$ is the conjugate of $Y_{mi}\dot{V}$.

Dividing both sides of equation (15) by $\dot{V}_m$ yields:

$$\frac{P_m + jQ_m}{\dot{V}_m} = \sum_{i=1}^{n} (Y_{mi}\dot{V}_i)^* \tag{16}$$

Express equation (16) as a simplified Taylor series expansion according to equation (13), namely:

$$(2 - \dot{V}_i)(P_m + jQ_m) \approx \sum_{i=1}^{n} (Y_{mi}\dot{V}_i)^* \tag{17}$$

$\sum_{i=1}^{n} (Y_{mi}\dot{V}_i)^*$ is the form resulting from multiplying the elements of the node admittance matrix by the node voltage phasors. Based on the principles governing the calculation of the admittance matrix and node voltages, this can be expanded into expressions for the admittances along the line and the corresponding node voltages, which can be expressed as:

$$(2 - \dot{V}_i)(P_m + jQ_m) \approx \sum_{i=1}^{n} (Y_{mi}\dot{V}_i)^* = \sum_{i \in X(m)} \left(\frac{\dot{V}_i - \dot{V}_m}{x_{mi}} \right)^* \tag{18}$$

In the equation, $X(m)$ denotes the set of nodes directly connected to node m.

Equations (13) and (18) are equations concerning voltage phasors. For any given voltage phasor $\dot{V}_i$, it can be expressed as:

$$\dot{V}_i = V_i(\cos\varphi_i + \mathrm{j}\sin\varphi_i) \tag{19}$$

In the equation, $V_i \sim \varphi_i$ represents the voltage amplitude and voltage phase of node i, respectively.

Expressing equations (13), (17), and (18) uniformly in matrix form:

$$\begin{bmatrix} B_r + C_r & -B_i + C_i \\ B_i + C_i & B_r - C_r \end{bmatrix} \begin{bmatrix} V_r \\ V_i \end{bmatrix} = \begin{bmatrix} S_r \\ S_i \end{bmatrix} \tag{20}$$

In the equation, B_r, C_r represents the simplified real-part coefficient; B_i, C_i represents the simplified imaginary-part coefficient; V_r, V_i denotes the real and imaginary parts of the voltage, respectively; S_r, S_r denotes the real and imaginary parts of the complex power, respectively.

As seen from equation (12), equation (20) is not a strict equality but rather an approximate expression. Therefore, introducing an error term into equation (20) yields:

$$\begin{bmatrix} B_r + C_r + \xi_r & -B_i + C_i + \omega_i \\ B_i + C_i + \omega_i & B_r - C_r + \xi_r \end{bmatrix} \begin{bmatrix} V_r \\ V_i \end{bmatrix} = \begin{bmatrix} S_r \\ S_i \end{bmatrix} \tag{21}$$

In the equation, ξ_r, ω_i represents the real-part and imaginary-part noise data, respectively.

2.2.3 Multi-Objective Ant Colony Distributed Solution Method

The multi-objective ant colony distributed algorithm is an algorithm within the edge computing framework. It sets an optimization objective within each cluster, simulating ants searching for the optimal food path within that cluster. The boundary coordination variables between multiple clusters serve as the information update quantities for ant colonies within each cluster. This algorithm features distributed computation, positive information feedback, and heuristic search capabilities, enabling distributed heuristic search for global optimization. It has been widely applied in fields such as distributed economic scheduling and fault analysis.

Traditional multi-objective ant colony algorithms suffer from issues like inefficient optimization processes and susceptibility to local optima. This paper proposes improvements based on the following approach: The foraging path of an ant seeking food is treated as the optimization process for state estimation within a single cluster. The collective optimization paths of the entire ant colony constitute the optimization process across multiple clusters. The ant that first locates food feeds back information as a cluster boundary coordination variable to other ants, and so on, ultimately enabling the entire colony to obtain food [47]. The solution process is as follows.

1) Express Equation (21) as the ant colony optimization model:

$$AX = b \tag{22}$$

$$A = \begin{bmatrix} B_r + C_r + \xi_r & -B_i + C_i + \omega_i \\ B_i + C_i + \omega_i & B_r - C_r + \xi_r \end{bmatrix} \tag{23}$$

$$X = [V_r \quad V_i]^T, b = [S_r \quad S_i]^T \tag{24}$$

2) Let the initial random search position for ants within the i cluster be:

$$\begin{aligned} X_K^i = \{0, & sum[2rand(K_1^i) - 1], \\ & sum[2rand(K_2^i) - 1], \cdots, \\ & sum[2rand(K_{max}^i) - 1]\} \end{aligned} \tag{25}$$

In the formula, X_K^i represents the estimated voltage state within the ind cluster; sum denotes the summation function, which calculates the total sum of ant paths; K_1^i corresponds to the first path iteration calculation within the ith cluster; similarly, $K_{\max}^i$ denotes the maximum path iteration calculation within the ith cluster; rand is the random calculation function, whose computational principle is:

$$\text{rand}(K) = \begin{cases} 1, \text{rand}(0,1) > 0.5 \\ 0, \text{rand}(0,1) \le 0.5 \end{cases} \tag{26}$$

In the formula, function $\text{rand}(K)$ corresponds to the expression in equation (23), with parameters K_1^i, etc.

3) Within each cluster, the ant colony follows the same solution process as in equation (23) to sequentially solve for the state estimation variable X (node voltage phasor) within each cluster. The path update rule for optimization is as follows:

$$K_i = \arg\max\left\{(q)^{\alpha}\left(\frac{1}{d_K}\right)^{\beta}\cdot\frac{1}{w^{\gamma}}\cdot\frac{1}{z^{\epsilon}}\right\} \tag{27}$$

In the formula: q represents the total information concentration released by ants during each iteration on path K; α denotes the importance value of the concentration on the ant's optimization path; β,γ,ε indicates the functional degree factor of the path heuristic; d_K signifies the optimization step distance of path K; w represents the time interval length; shorter intervals indicate denser and more critical computations; z denotes the state estimation error; lower errors indicate higher information concentration on the ant-optimization path, necessitating optimization along that path.

4) The feedback update for cluster boundary nodes is expressed as:

$$\begin{cases} q_K(t+1) = (1-p)q_K(t) + \dfrac{q_K(t)}{l_K(t)} + \zeta f_K(t) \\ f_K(t+1) = \mu f_K(t)[1-f(t)] \end{cases} \tag{28}$$

In the formula, f_K represents the amount of path information obtained by Logistic chaotic mapping; Both $t, t+1$ represent the number of iterative updates; ζ is the update coefficient, which is set according to the system environment. μ is the indicator factor of the iteration direction, with a value range of [3.0, 3.5]; $l_K(t)$ is the iteration moment step size of t.

The above steps can greatly enhance the speed and efficiency of the solution. The solution process is shown in Figure 1.

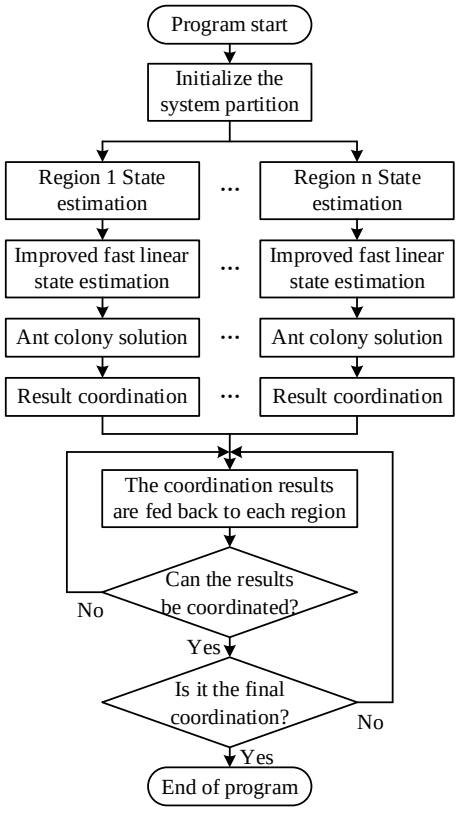

Figure 1: shows the distributed state estimation process proposed in this paper

2.3 Experimental Results and Analysis

To validate the effectiveness of the proposed real-time state estimation method for distribution networks, this section develops a test program within the MATLAB 2022b environment. Analysis is conducted using the operation optimization of an enhanced IEEE 33-node system as an example. The IEEE 33-node topology is illustrated in Figure 2. As shown, photovoltaic power generation systems and wind turbines are connected to nodes 13 and 30, respectively.

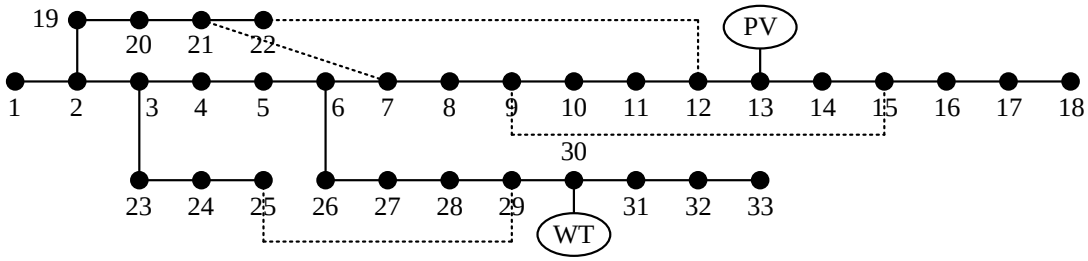

Figure 2: Improved IEEE 33 node topology diagram

2.3.1 State Estimation Testing Under Normal Conditions

Node 8 in the modified IEEE 33-node system was selected as the observation node to compare state estimates obtained using traditional centralized least squares with the proposed algorithm. Figure 3 details the comparison between estimated and true values for voltage magnitude and phase angle at each time step for Node 8. Figures (a) and (b) correspond to voltage magnitude and phase angle, respectively. The figures reveal that the voltage estimates based on the least squares method exhibit significant deviations from the true values, indicating substantially inferior estimation performance compared to the proposed algorithm. Under normal operating conditions, the proposed algorithm demonstrates superior state estimation capability.

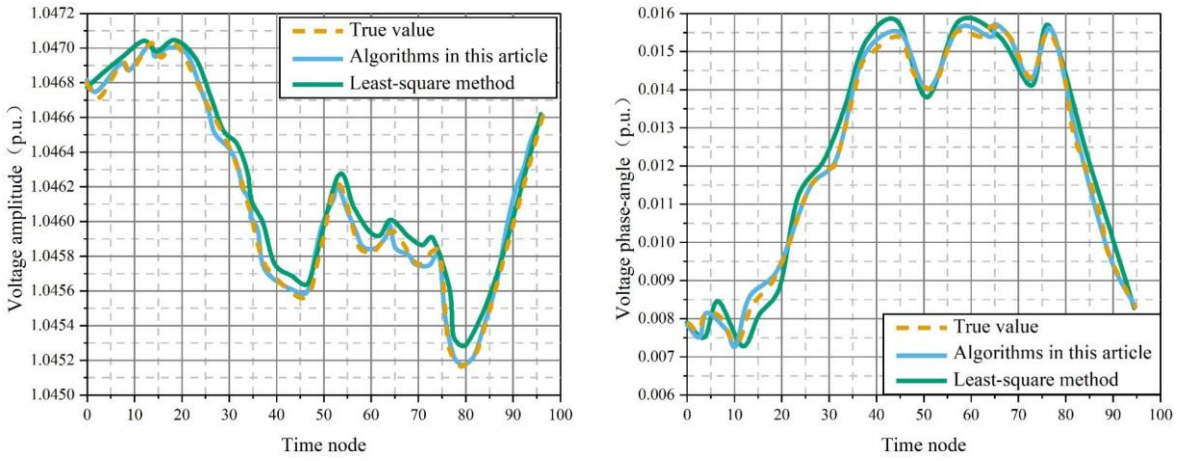

(a)Voltage amplitude (b)Voltage phase-angle

Figure 3: Comparison of estimated and true values of voltage amplitude and phase angle

To enable a more intuitive comparison of the estimation capabilities between the least squares method and the proposed algorithm, the estimation accuracy of both methods will be analyzed by comparing the errors between the true and estimated voltage values. The accuracy of state estimation is characterized by the absolute errors between the true and estimated voltage values at each time instant. The errors in voltage magnitude and phase angle at node 8 for each time instant are shown in Figure 4. Figures (a) and (b) correspond to voltage magnitude and

phase angle, respectively. It is evident that the deviations in voltage magnitude and phase angle for the proposed algorithm are predominantly smaller than those of the least squares method. Under normal operating conditions of distribution networks, the proposed algorithm can accurately and effectively estimate the voltage magnitude and phase angle at each node. The errors between the estimated values and the true values are significantly smaller than those of the least squares method, demonstrating higher precision. Therefore, under normal circumstances, the proposed state estimation algorithm exhibits superior dynamic estimation capability and higher estimation accuracy.

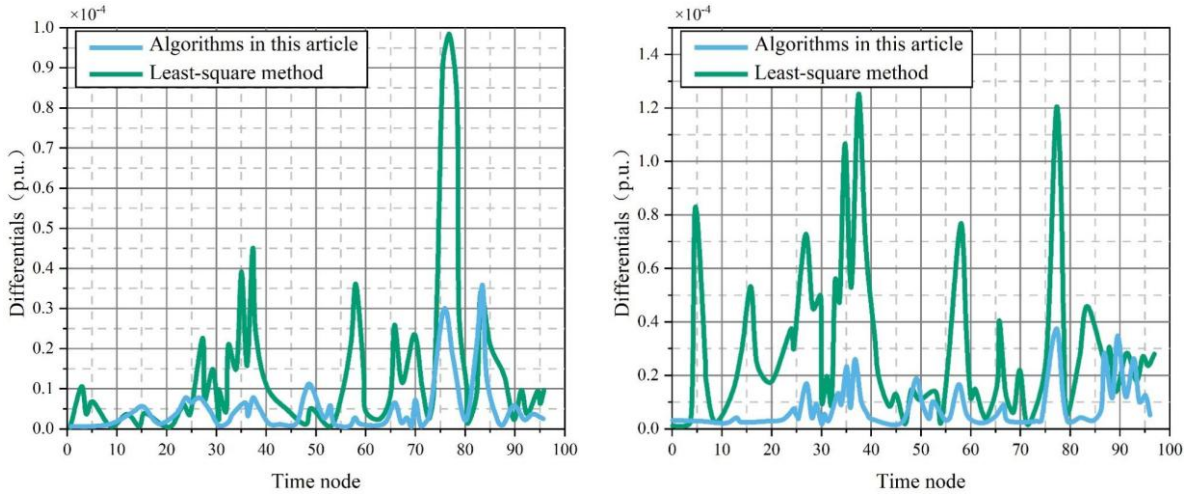

(a)Voltage amplitude (b)Voltage phase-angle

Figure 4: Comparison of the difference between voltage amplitude and phase angle

2.3.2 State Estimation Testing Under Adverse Data Conditions

Under normal circumstances, when measurement data errors exceed a certain threshold (e.g., surpassing a predetermined value), the measurement data is classified as bad data. In practical distribution network sensor data collection, the proportion of bad data is approximately 2%. To simulate scenarios where bad data may occur in distribution networks, this paper continues to use Node 8 in the IEEE 33-node system as the observation point. During the sampling period from 100 to 160, observation noise ranging from 2 to 5 times the original signal is injected into the observed data. The relative errors in voltage magnitude and phase angle between the least squares method and the proposed algorithm are shown in Figure 5. Figures (a) and (b) correspond to voltage magnitude and phase angle, respectively. The figures demonstrate that the proposed algorithm achieves significantly superior estimation performance for the distribution network system state compared to the least squares method when corrupted data is present.

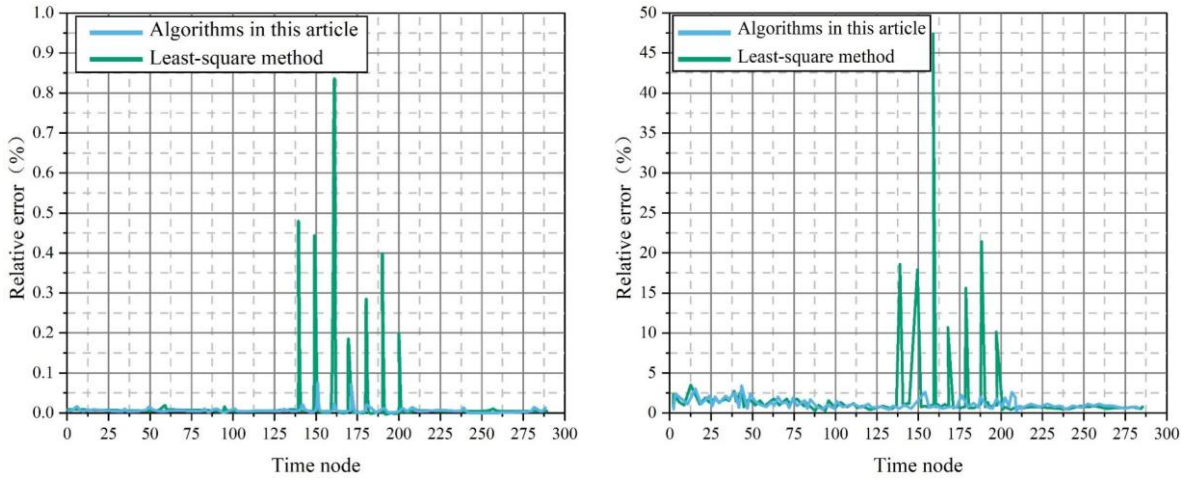

(a)Voltage amplitude (b)Voltage phase-angle

Figure 5: The relative error of voltage amplitude and phase angle of No.8 node

2.3.3 State Estimation Testing Under Load Transient Conditions

This section assumes that during operation of the enhanced IEEE 33-node system, node 10 experiences a sudden surge in load at a specific moment—such as disorderly access of electric vehicles—causing a substantial short-term increase in distribution network load. The load at node 10 abruptly jumps from 0.0043 (p.u.) to 0.096 (p.u.). When the load at node 10 undergoes this abrupt change, the actual values of voltage magnitude and phase angle at node 10 during the system disturbance, along with the state estimates from the proposed algorithm and the least squares method, are shown in Figure 6. Figures (a) and (b) correspond to voltage magnitude and phase angle, respectively. During load transients, the state estimates from the proposed algorithm more closely approach the true values, better reflecting the system's dynamic changes. Evidently, the proposed algorithm demonstrates superior adaptability to load transients in distribution systems, enabling more accurate state estimation for distribution networks.

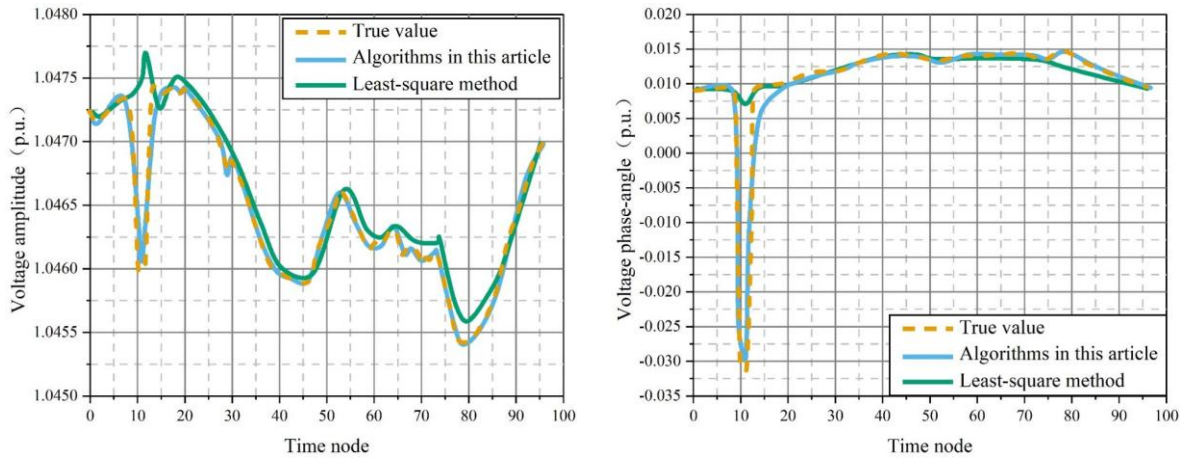

(a)The voltage amplitude at node 10 (b)Voltage phase angle at node 10

Figure 6: The voltage amplitude and voltage phase angle at node 10

3 Edge-Based Security Detection Model for Distribution Networks

As power systems evolve toward intelligent and digital solutions, traditional distribution network safety inspection methods—characterized by slow fault detection, insufficient data collection accuracy, and imprecise fault localization—no longer meet modern grid requirements for efficiency, precision, and real-time responsiveness. To achieve precise and rapid fault detection within distribution networks, enabling comprehensive safety monitoring and early warning systems, this chapter will establish a distribution network safety inspection model based on edge computing. This model will effectively address the diverse topological structures inherent in distribution network configurations.

3.1 Edge-Based Feature Extraction for Distribution Networks

Edge computing resides between physical entities and industrial connections, or at the top of physical entities. Meanwhile, cloud computing can still access historical data from edge computing. The method described in this paper utilizes a 5G network channel: after the fault detector uploads real-time voltage data from the power grid to the edge side, the edge side implements detector control. Based on the edge side, a multidimensional S-transform fusion algorithm combined with the Sagami transform matrix method extracts relevant fault features. To facilitate further processing of these features and enable customers to locate detector access interfaces more conveniently and rapidly, the data is uploaded in parallel to a proxy server.

The implementation flow for fault feature extraction in distribution networks based on the edge side is shown in Figure 7. Customers can access suspected fault information and visualization data for distribution networks by reviewing and managing various terminal devices. A website developed using ASP.NET displays the operational status of the distribution network and detectors, addressing latency issues across different edge servers. The server promptly retrieves grid data collected by the ADS8365W5300 chip, transmits it to the server center, and presents it through real-time waveform recording. Detectors automatically transmit acquired fault data to the server database for storage and archiving.

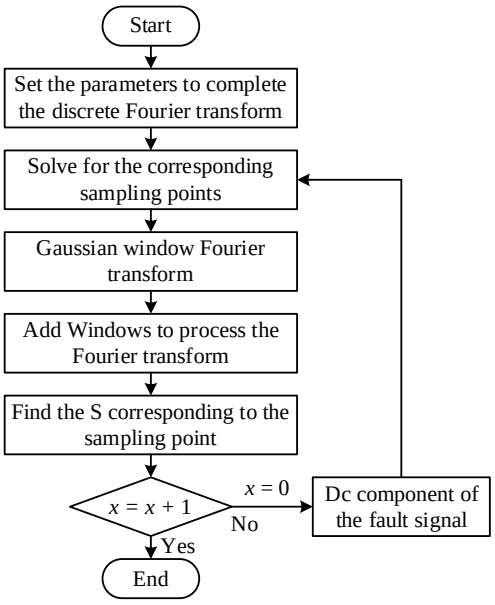

Figure 7: Fault feature extraction process of distribution networks

Based on Figure 7, a more specific calculation method is elaborated as follows:

1) Assuming the sampling time interval of the power grid data is T, the total number of samples is X, and the discrete sampling sequence of the continuous voltage signal $h(t)$ is $h(lT)$, then the discrete Fourier transform of the continuous voltage signal $h(t)$ is as follows [48]:

$$H\left(\frac{x}{XT}\right)=\frac{1}{X}\sum_{\iota=0}^{X-1}h(lT)\exp\left(\frac{-\varphi^2\pi x\iota}{X}\right) \tag{29}$$

In the formula: x denotes the ordinal number of the sampling point, with a value of $0,1,\cdots,X-1$; φ is the imaginary unit.

Assuming only one sampling point, the corresponding discrete Fourier transform is obtained by solving the above equation.

2) Using the following formula, calculate the Fourier transform $F(y,x)$ of the Gaussian window f corresponding to sampling point x:

$$F(y,x)=\exp\left(\frac{-2\pi^2y^2}{f^2x^2}\right) \tag{30}$$

In the equation: γ represents the step size of the Gaussian window.

3) After shifting $H\left(\frac{y}{XT}\right)$ to position $H\left(\frac{x+y}{XT}\right)$, apply windowing to $H\left(\frac{x+y}{XT}\right)$ using the following expression to obtain the new Fourier transform as shown in Equation (31):

$$B(y,x)=H\left(\frac{x+y}{XT}\right)*F(y,x) \tag{31}$$

4) After performing the inverse Fourier transform, obtain the S-transform row vector $\left[\frac{x}{XT},kT\right]$ corresponding to sampling point x. Here, k is an arbitrary constant with a value of $0,1,\cdots,X-1$.

5) Let $x=x+1$. Iterate the first four steps until S-transform row vectors for all sampling points are obtained, then terminate the calculation. If $x=0$, use the following equation to obtain the S-transform row vector [0, kT], which serves as the DC component of the fault signal:

$$[0,kT]=\frac{1}{X}\sum_{y=0}^{X-1}H\left(\frac{y}{XT}\right) \tag{32}$$

During fault detection, the impedance matrix of the line requires decoupling processing, i.e., achieving diagonalization of the impedance matrix. Therefore, the Sogo transformation matrix method is adopted as the analysis strategy for the edge side. Assuming the characteristic matrix of line impedance matrix z is η, representing the decoupled magnitude impedance, then the Sogo transformation matrix s satisfies the following equation:

$$s^{-1}zs=\eta \tag{33}$$

Its line impedance matrix z is defined by the following expression.

$$z = \begin{bmatrix} z_{q1} & z_{\mu 1} & z_{\mu 2} \\ z_{\mu 1} & z_{q2} & z_{\mu 3} \\ z_{\mu 2} & z_{\mu 3} & z_{q3} \end{bmatrix} \tag{34}$$

Among these, the self-impedance and mutual impedance of each phase are z_{q1}, z_{q2}, z_{q3} and $z_{\mu 1}, z_{\mu 2}, z_{\mu 3}$, respectively.

Using the symmetrical component method to perform decoupling, the following matrix is obtained.

$$s = \begin{bmatrix} 1 & 1 & 1 \\ \alpha^2 & \alpha & 1 \\ \alpha & \alpha^2 & 1 \end{bmatrix} \tag{35}$$

In the formula, α is the rotation factor. Combining the above three equations, the eigenvalue matrix η is obtained, representing the impedance parameters of different orders.

3.2 Fault Detection in Distribution Networks

The nodes in the distribution network topology correspond to the detection devices within the edge computing model. The lines between adjacent detection devices represent structural branches. The detection device-branch association matrix L describes the relationships between nodes and branches. The network topology of the target distribution network is described using the matrix form based on the detection device-branch association matrix L.

Given that the number of branches equals the number of detection devices, if the edge computing model contains m detection devices, then the matrix dimension of the detection device-branch association matrix L is m. Therefore, for the detection device-branch association matrix L, the following conditional equations define its matrix elements l_{ij} where the detection device is i and the branch is j:

$$l_{ij} = \begin{cases} 1 & i \text{ is directly connected to } j \text{ and } j \text{ is in the positive direction of } i \\ 0 & i \text{ and } j \text{ are not directly connected} \\ -1 & i \text{ is directly connected to } j \text{ and } j \text{ is in the opposite direction of } i \end{cases} \tag{36}$$

The positive direction of this equation is defined as the path originating from the system power source and terminating at the distributed power source within the distribution network. This directional specification ensures that the capacity and connection point of the distributed power source possess a certain degree of immunity to interference in fault positive direction detection, thereby enhancing the reliability and sensitivity of the detection results.

Assuming a fault occurs in a power distribution network, the fault information collected by the i detection device is g_i. Complete the value according to the following conditional equation:

$$g_i = \begin{cases} 1 & \text{A fault current has been detected and its direction is positive} \\ 0 & \text{No fault current was detected} \\ -1 & \text{A fault current was detected and its direction was in the opposite direction} \end{cases} \tag{37}$$

When the contact switch is in the closed state, only the fault direction needs to be identified. Using the following logical expression, the corrected fault information $g_i^{'}$ is obtained by processing the detected fault information g_i and 1 through synchronous processing:

$$g_i^{'} = \overline{g_i \oplus 1} \tag{38}$$

The corrected fault information values are all 0. Fault information $g_i^{'}$, which adopts a value of 0, is used to construct the $1*m$-order fault information matrix G. The product of this matrix and the detection device-branch correlation matrix L yields the fault section information matrix P, indicating the location of the fault. Its mathematical expression is as follows:

$$P = G*L \tag{39}$$

If an element in this matrix takes the value 1, it indicates that the position corresponding to that matrix element belongs to a faulted section.

Assuming the distribution network contains ten sections, line A in section $a_1 \sim a_{10}$ is in normal operation with the tie switch open. The element values in the detection device-branch association matrix L for this line are determined as shown in Equation (40):

$$L = \begin{bmatrix} -1 & 0 & 0 & 0 & 0 & 0 & 0 & 0 & 0 & -1 \\ -1 & 1 & 0 & 0 & 0 & 0 & 0 & 0 & 0 & 0 \\ 0 & -1 & 1 & 0 & 0 & 0 & 0 & 0 & 0 & 0 \\ 0 & 0 & -1 & 1 & 0 & 0 & 0 & 0 & 0 & 0 \\ -1 & 0 & 0 & 0 & 1 & 0 & 0 & 0 & 0 & 0 \\ 0 & -1 & 0 & 0 & 0 & 1 & 0 & 0 & 0 & 0 \\ 0 & 0 & -1 & 0 & 0 & 0 & 1 & 0 & 0 & 0 \\ -1 & 0 & 0 & 0 & 0 & 0 & 0 & 1 & 0 & 0 \\ 0 & -1 & 0 & 0 & 0 & 0 & 0 & 0 & 1 & 0 \\ 0 & 0 & -1 & 0 & 0 & 0 & 0 & 0 & 0 & 1 \end{bmatrix} \tag{40}$$

The element values of the corrected fault information matrix G are obtained as shown in Equation (41):

$$G = \begin{bmatrix} 1 & 1 & 1 & 0 & 0 & 0 & 0 & 0 & 1 & 1 \end{bmatrix} \tag{41}$$

Using Equation (39), calculate the fault section information matrix P. When an element in the fault section information matrix is 1, a fault is determined to have occurred, yielding the element value result shown in Equation (42):

$$P = \begin{bmatrix} 0 & 0 & 1 & 0 & 0 & 0 & 0 & 0 & 0 & 0 \end{bmatrix} \tag{42}$$

The ten elements in Matrix P correspond to the ten segments of the transmission line. Based on the value of the third column element, a fault is detected in Segment a_3 of Line A, completing the fault detection process.

3.3 Experimental Results and Analysis

3.3.1 Comparative Analysis of Performance Metrics

To objectively evaluate the performance metrics of the models, this experiment compares the security detection algorithm proposed in this chapter with security detection algorithms based on ELM, Petri, and XGBoost. For better comparison, this subsection assesses each model using accuracy, precision, recall, and F1-score. To enhance the feasibility of the experiment, the average of 10 repeated trials is taken for each model. The diagnostic results comparison of different distribution network security detection models is shown in Table 1. As indicated, the proposed model achieves higher accuracy and precision among the four models, reaching 94.16% and 94.68%, respectively. However, its recall value is still comparatively moderate. On analyzing the same in detail through F1-score, one finds that the suggested model outshines others in terms of capability, with an F1-score of 93.7%.

Table 1: Diagnosis results of different distribution network security detection models

Method model	Accuracy rate	Precision rate	Recall rate	F1-score
The method of this paper	94.16%	94.68%	90.44%	93.70%
ELM	92.09%	93.77%	89.37%	91.12%
Petri	90.18%	93.47%	89.01%	90.67%
XGBoost	91.49%	93.71%	93.12%	92.92%

3.3.2 Interference Immunity Analysis

Environmental disturbances are common in practical distribution network systems, including operation processes that include both engaging and disengaging loads and capacitors. Such disturbances can cause measured voltage and current waveform signals to have a poorer quality than simulated idealized data. To confirm the validity of the suggested algorithm in real distribution networks, simulation raw signals were created using the MATLAB simulation environment. White noise interference was then added to the test sample set by varying the signal-to-noise ratios (SNR) by 5dB, 10dB, 15dB, 20dB, 25dB, and 30dB. Table 2 contains a detailed description of the model accuracy at various signal-to-noise ratios. The test findings show that the accuracy of the given model on the test set is gradually reduced as the signal-to-noise ratio goes down. It is so because the signal-to-noise ratio is the ratio of signal to noise and the greater the ratio, the greater signal component and less noise interference is present and thus the signal quality is improved and the accuracy is increased. In particular, at 5dB SNR, the test set is at the lowest accuracy of the model with a reduction of about 3% over the no-noise case. But the general decline is still gentle. Despite the changes in SNR, the proposed model has always been more accurate than the other comparison models. This shows that the model is very resistant to interference and can be used to solve complicated situations like noise interference in the real-life power distribution networks.

Table 2: Model accuracy for different SNRS

SNRS(dB)	Accuracy(%)			
	The method of this paper	ELM	Petri	XGBoost
5	91.26	75.32	81.45	72.42
10	91.82	77.5	84.14	73.63
15	92.34	78.7	86.84	74.36
20	92.83	79.11	87.88	76.25
25	93.22	80.22	88.31	78.66
30	93.67	80.69	88.87	79.45

4 Real-Time Status Estimation and Safety Early Warning System for Distribution Networks

Due to the steady growth of power systems, conventional solutions to estimating the real-time state and predicting the safety of distribution grids are unable to keep up with the ever-changing operating conditions of contemporary power grids. The paper develops an IoT-based real-time status estimation and safety early warning system of distribution grids. Its functional implementation principles include the use of proposed edge-based algorithms to estimate the real-time status and detect the safety models. Starting the process of data acquisition and transmission to the end of processing, the system is able to monitor the operational status and diagnose faults of distribution grids.

4.1 System Hardware Architecture Design

The hardware architecture is the basis of the distribution network automation monitoring system that will provide effective data acquisition, transmission and processing as a result of the rational structure of different modules. The IoT-based distribution network automation monitoring system hardware architecture is depicted in Figure 8. All the hardware architecture of the entire system involves sensor nodes, data acquisition terminals, edge computing gateways and cloud servers. The components all operate closely together to ensure the complete monitoring and control of the operational condition of the distribution network.

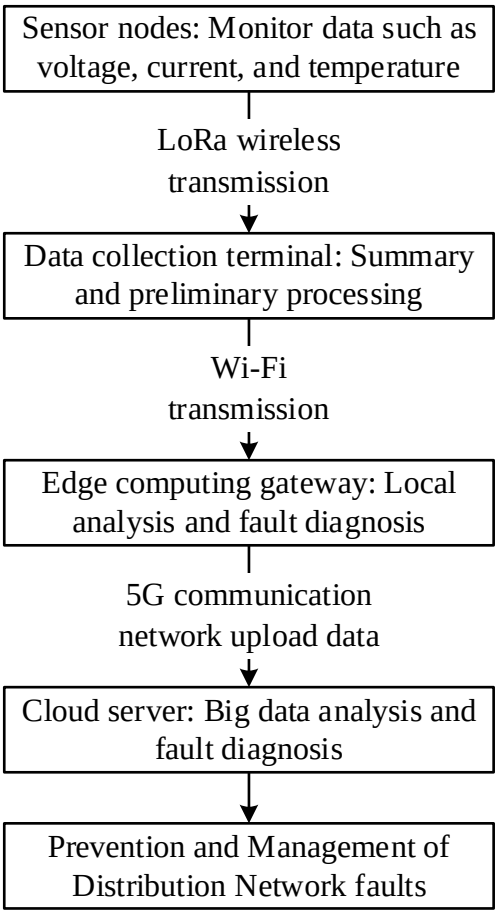

Figure 8: Hardware architecture of distribution network automation monitoring system

4.1.1 Sensor Node

The sensor nodes are installed in important places across the power distribution systems, which allow monitoring electrical parameters (voltage, current, and power) in real-time and detecting environmental parameters (temperature and humidity). In particular, the design uses the STM32F103 low-power microcontroller and a LoRa wireless communication module to attain long-distance and low-power data acquisition and transmission. SDP31 temperature and humidity sensors and ACS712 current sensors are used in sensor nodes to provide high-precision parameter measurements in a complicated power environment. The design of the nodes focuses on minimizing energy consumption and ensuring maximum range of communication, hence providing the ability to transmit data at high rates and stably to the data acquisition terminal.

4.1.2 Data Acquisition Terminal

The data acquisition terminal is based on a Raspberry Pi 4B as the central device, which is used to collect data of sensor nodes and perform initial processing. With a high-performance Broadcom BCM2711 quad-core processor, this terminal is capable of compressing incoming data and encrypting it using the AES-256 algorithm to protect the data security and integrity at the time of transmission. The terminal is equipped with a dual-antenna Wi-Fi module that supports high-speed wireless transmission to reduce the latency and increase the transmission efficiency. It also uses USB interfaces to connect to sensor nodes, and thus allows backup transmission through wire.

4.1.3 Edge Computing Gateway

The edge computing gateway is designed using the NVIDIA Jetson Nano computing device as the processing core of the system. Using the 5G wireless communication module, data can be transmitted to cloud-based servers at very low latencies without increasing the computational burden of the cloud server.

4.2 System Software Functionality Implementation

The system software functions are closely related to the hardware architecture. Core components of the software functional modules include data acquisition, data transmission, state estimation, safety alerts.

4.2.1 Data Acquisition Module

The data acquisition module works on an asynchronous method of collecting data based on an interrupt-driven technique. In this regard, as soon as the data is collected by each sensor node, the system triggers an interrupt, allowing the data to be transferred to the main control unit without loss.

4.2.2 Data Transmission Module

The data transmission module is communicated over WSN through lightweight and efficient Message Queue Telemetry Transport (MQTT) protocol in order to provide stable transmission with low bandwidth. The sensor nodes package the data collected on them and send it to edge computing gateways. Once data is received by the gateway, it will be compressed first as a way to minimize transmission size and make it more efficient. Then, the compressed data is encrypted with the AES-256 algorithm to prevent the interception and tampering of the data in transit.

4.2.3 State Estimation Module

Employing the edge-based algorithm model for real-time state estimation of distribution networks developed in this paper, we perform real-time analysis and state monitoring of massive distribution network data. By utilizing a multi-objective ant colony distributed algorithm, we rapidly obtain state results both within clusters and across the entire distribution network, thereby completing preparatory work for distribution network security inspections.

4.2.4 Safety Alert Module

The fault diagnosis module employs the edge-based distribution network safety detection model proposed in this paper. It constructs a fault information matrix to obtain fault section data, then determines faults on line segments based on specified threshold conditions. This process completes fault detection within the distribution network and issues early warnings.

4.3 Case Study Analysis

This section will conduct practical testing of the real-time status estimation and safety early warning system for distribution networks established in this paper. The field experiment utilized armored underground cables from a three-feeder 380V distribution system at a certain facility. Data collection was performed at the feeder-end substation boxes using Raspberry Pi 4B devices.

4.3.1 Data Acquisition Accuracy Comparison

This paper compares the data acquisition method employed by the proposed system with the traditional approach, which directly connects the address bus to both the flash memory and RAM devices (referred to as the “traditional acquisition method”). Figure 9 illustrates the electromagnetic interference simulation results for the proposed system versus the traditional acquisition method. Figures (a) and (b) correspond to the traditional acquisition method and the proposed system, respectively. The simulation results demonstrate that the electromagnetic interference values remain below the maximum tolerable level for the proposed system, leaving a margin of safety. This ensures the system's normal operation even under unexpected conditions, significantly outperforming the traditional acquisition method.

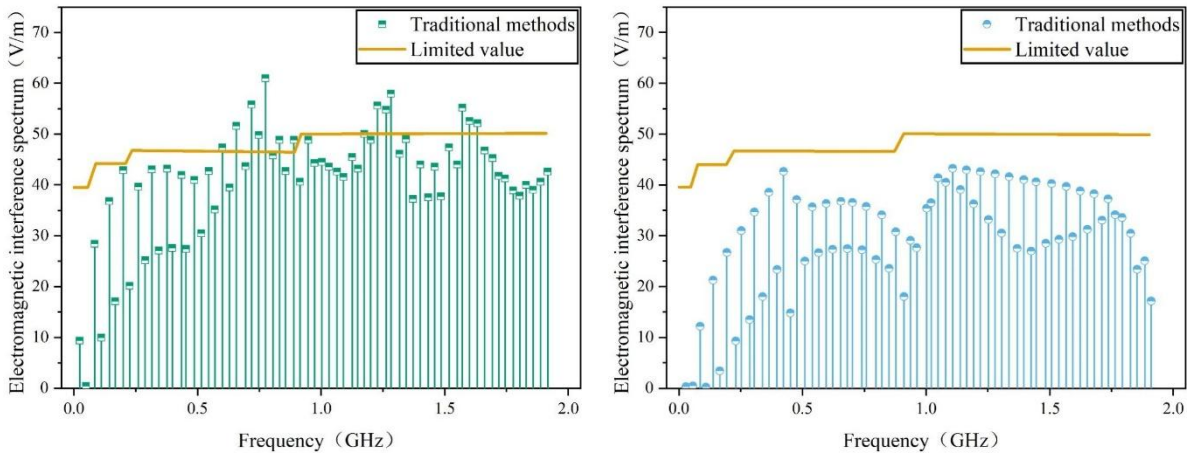

(a)Traditional collection methods (b)The system of this article

Figure 9: Electromagnetic interference simulation diagram

4.3.2 Analysis of System Inspection Results

Using the system described in this paper to process the feeder lines of the tested cables, preliminary results indicate that the zero-sequence current amplitude of Feeder 1 is significantly greater than that of Feeder 2. The instantaneous energy distribution diagrams for Feeder 1 and Feeder 2 are shown in Figure 10. Figures (a) and (b) correspond to Feeders 1 and 2, respectively. It can be roughly determined that changes occur in the range of 4000 to 5000 points for both Feeders 1 and 2.

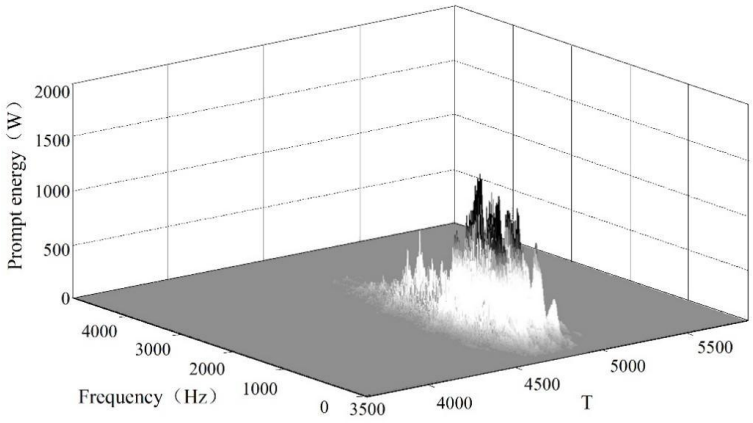

(a)Feeder 1

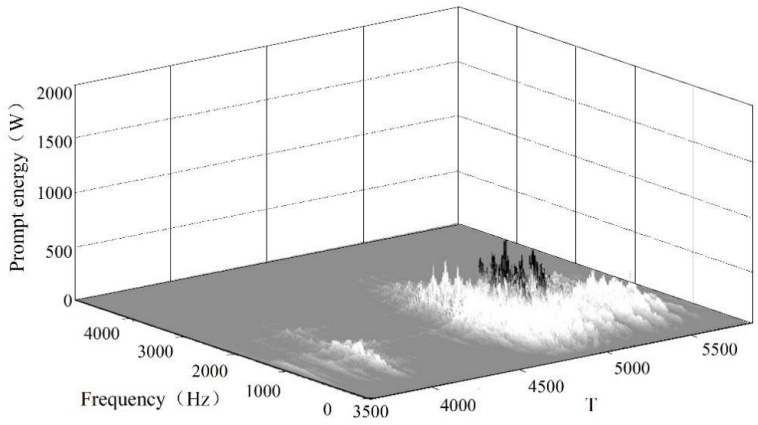

(b)Feeder 2

Figure 10: Instantaneous energy distribution diagram

For ease of observation, feeders 1 and 2 were processed, with their time-domain instantaneous energy distribution plots shown in Figure 11. Figures (a) and (b) correspond to feeders 1 and 2, respectively. The figures reveal that the onset of instantaneous energy rise in feeder 2 is significantly delayed compared to feeder 1. Verification against actual conditions confirms that the longer distribution lines in feeder 2 cause a time lag in propagating fault energy from feeder 1 to feeder 2. The detection results of this system align with real-world observations.

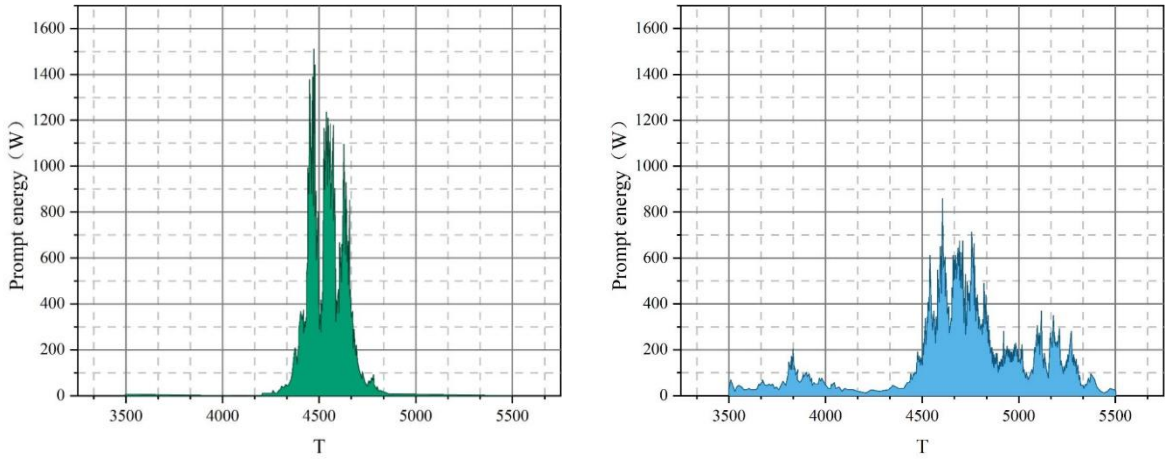

(a)Feeder 1 (b)Feeder 2

Figure 11: The instantaneous energy curve

Through calculation, the correctness weights for feeders 1–3 were determined to be 0.663, 0.175, and 0.166, respectively. Therefore, feeder 1 was identified as the faulty feeder. After maintenance, the identified faulty feeder was confirmed to be feeder 1. The cause of the fault was insulation damage exposing the cable, accompanied by significant partial discharge phenomena. The field-collected data, processed through the system described in this paper, enables accurate condition estimation and safety alerts for actual power lines, demonstrating promising practical application prospects.

5 Conclusion

This paper proposes a multi-objective ant colony distributed solution algorithm for edge computing to achieve real-time state estimation of distribution networks. Using the operation optimization of an improved IEEE 33-node system as an example, state estimation experiments were conducted. Under normal conditions, corrupted data, and load sudden changes, both the voltage magnitude and phase angle estimates from this algorithm closely match true values, demonstrating significantly superior state estimation performance compared to the contrasted least squares algorithm. Based on edge computing, a security detection model for distribution networks is constructed to enable security monitoring and fault diagnosis. Compared with security detection algorithms based on ELM, Petri, and XGBoost, the proposed algorithm exhibits moderate recall but achieves the highest accuracy, precision, and F1-score at 94.16%, 94.68%, and 93.7%, respectively. Regarding interference resistance, the accuracy of this safety detection model consistently outperformed other comparison models across varying signal-to-noise ratios, demonstrating outstanding interference resilience. Finally, based on the proposed edge-based real-time state estimation and safety detection models for distribution networks, a real-time state estimation and safety early warning system for distribution networks under an IoT framework was constructed. This system was applied to perform state estimation and safety detection on a three-feeder armored buried cable at a certain facility. This detection result showed that the faulty feeder was Feeder 1 which is as expected. This illustrates the usefulness of the suggested system along with its good opportunities of use in the field of the on-line state estimation and safety early warning of distribution networks.

Funding

This research was supported by the Natural Science Foundation of Fujian Province: The Logical and Practical Path of Digital Enabling High-quality Development of Fujian Cultural Tourism Industry (number: 2023J05213);

This research was supported by the Philosophy and Social Sciences Project of Guangdong Province: Research on the Internal Mechanism and Practical Path of the New Development Pattern of Domestic and International Double Cycle Enabled by Digital Technology (Number: GD23XYJ03).

References

[1] Anastasiadis, A. G., Kondylis, G. P., Polyzakis, A., & Vokas, G. (2019). Effects of increased electric vehicles into a distribution network. Energy Procedia, 157, 586-593.

[2] Caballero-Pena, J., Cadena-Zarate, C., Parrado-Duque, A., & Osma-Pinto, G. (2022). Distributed energy resources on distribution networks: A systematic review of modelling, simulation, metrics, and impacts. International Journal of Electrical Power & Energy Systems, 138, 107900.

[3] Stecca, M., Elizondo, L. R., Soeiro, T. B., Bauer, P., & Palensky, P. (2020). A comprehensive review of the integration of battery energy storage systems into distribution networks. IEEE Open Journal of the Industrial Electronics Society, 1, 46-65.

[4] Yang, X., Xu, C., He, H., Yao, W., Wen, J., & Zhang, Y. (2020). Flexibility provisions in

active distribution networks with uncertainties. IEEE Transactions on Sustainable Energy, 12(1), 553-567.

[5] Mlilo, N., Brown, J., & Ahfock, T. (2021). Impact of intermittent renewable energy generation penetration on the power system networks–A review. Technology and Economics of Smart Grids and Sustainable Energy, 6(1), 25.

[6] Sun, W., Neumann, F., & Harrison, G. P. (2020). Robust scheduling of electric vehicle charging in LV distribution networks under uncertainty. IEEE Transactions on Industry Applications, 56(5), 5785-5795.

[7] Sharma, S., Niazi, K. R., Verma, K., & Rawat, T. (2020). Impact of battery energy storage, controllable load and network reconfiguration on contemporary distribution network under uncertain environment. IET Generation, Transmission & Distribution, 14(21), 4719-4727.

[8] Liu, M., Phanivong, P. K., Shi, Y., & Callaway, D. S. (2017). Decentralized charging control of electric vehicles in residential distribution networks. IEEE Transactions on Control Systems Technology, 27(1), 266-281.

[9] Bahramara, S., Mazza, A., Chicco, G., Shafie-khah, M., & Catalão, J. P. (2020). Comprehensive review on the decision-making frameworks referring to the distribution network operation problem in the presence of distributed energy resources and microgrids. International Journal of Electrical Power & Energy Systems, 115, 105466.

[10] Kazmi, S. A. A., Shahzad, M. K., Khan, A. Z., & Shin, D. R. (2017). Smart distribution networks: A review of modern distribution concepts from a planning perspective. Energies, 10(4), 501.

[11] Chen, F., Xu, W. W., Wang, Z. H., Yang, T., & Huang, H. Y. (2021). A research on early warning method of Distribution Network Cyber Physical System. In E3S Web of Conferences (Vol. 248, p. 02054). EDP Sciences.

[12] Xu, J., Jin, Y., Zheng, T., & Meng, G. (2023). On state estimation modeling of smart distribution networks: a technical review. Energies, 16(4), 1891.

[13] Vijaychandra, J., Prasad, B. R. V., Darapureddi, V. K., Rao, B. V., & Knypiński, Ł. (2023). A review of distribution system state estimation methods and their applications in power systems. Electronics, 12(3), 603.

[14] Ajoudani, M., Sheikholeslami, A., & Zakariazadeh, A. (2020). Modified weighted least squares method to improve active distribution system state estimation. Iranian Journal of Electrical and Electronic Engineering, 16(4), 559-572.

[15] Ling, W. A. N. G., Zhi, D. E. N. G., Ming, M. A., Xin, W. A. N. G., & Dong-hai, Y. A. N. G. (2020, September). A Weight Least Square State Estimation Based Fault Location For Distribution Network. In 2020 12th IEEE PES Asia-Pacific Power and Energy Engineering Conference (APPEEC) (pp. 1-5). IEEE.

[16] Ferreira, D. M., Carvalho, P. M., & Ilić, M. D. (2024). A Kalman filter approach for state estimation in weakly monitored active distribution networks. Sustainable Energy, Grids

and Networks, 39, 101423.

[17] Kettner, A. M., & Paolone, M. (2017). Sequential discrete Kalman filter for real-time state estimation in power distribution systems: Theory and implementation. IEEE Transactions on Instrumentation and Measurement, 66(9), 2358-2370.

[18] Wu, J., Lin, K., Wu, F., Wang, Z., Shi, L., & Li, Y. (2023). Improved unscented Kalman filter based interval dynamic state estimation of active distribution network considering uncertainty of photovoltaic and load. Frontiers in Energy Research, 10, 1054162.

[19] Wang, K., Liu, M., He, W., Zuo, C., & Wang, F. (2022). Koopman Kalman particle filter for dynamic state estimation of distribution system. IEEE Access, 10, 111688-111703.

[20] Watitwa, J. K., & Awodele, K. O. (2020, August). Active distribution system state estimation: comparison between weighted least squares and extended kalman filter algorithms. In 2020 IEEE PES/IAS PowerAfrica (pp. 1-5). IEEE.

[21] Kumari, N., Kulkarni, R., Ahmed, M. R., & Kumar, N. (2021). Use of kalman filter and its variants in state estimation: A review. Artificial intelligence for a sustainable industry 4.0, 213-230.

[22] Ye, L., Woodford, N., Roy, S., & Sundaram, S. (2020). On the complexity and approximability of optimal sensor selection and attack for Kalman filtering. IEEE Transactions on Automatic Control, 66(5), 2146-2161.

[23] Jin, X. B., Robert Jeremiah, R. J., Su, T. L., Bai, Y. T., & Kong, J. L. (2021). The new trend of state estimation: From model-driven to hybrid-driven methods. Sensors, 21(6), 2085.

[24] Huang, M., Wei, Z., Sun, G., & Zang, H. (2019). Hybrid state estimation for distribution systems with AMI and SCADA measurements. IEEE Access, 7, 120350-120359.

[25] Wang, G., Giannakis, G. B., Chen, J., & Sun, J. (2019). Distribution system state estimation: An overview of recent developments. Frontiers of Information Technology & Electronic Engineering, 20(1), 4-17.

[26] Zamzam, A. S., Fu, X., & Sidiropoulos, N. D. (2019). Data-driven learning-based optimization for distribution system state estimation. IEEE Transactions on Power Systems, 34(6), 4796-4805.

[27] Liu, Y., Wang, Y., & Yang, Q. (2023). Spatio-temporal generative adversarial network based power distribution network state estimation with multiple time-scale measurements. IEEE Transactions on Industrial Informatics, 19(9), 9790-9797.

[28] Džafić, I., & Jabr, R. A. (2017). Real time multiphase state estimation in weakly meshed distribution networks with distributed generation. IEEE Transactions on Power Systems, 32(6), 4560-4569.

[29] Liu, Y., Li, J., & Wu, L. (2019). State estimation of three-phase four-conductor distribution systems with real-time data from selective smart meters. IEEE Transactions on Power Systems, 34(4), 2632-2643.

[30] Manousakis, N. M., & Korres, G. N. (2021). Application of state estimation in distribution systems with embedded microgrids. Energies, 14(23), 7933.

[31] Soltani, Z., & Khorsand, M. (2022). Real-time topology detection and state estimation in distribution systems using micro-PMU and smart meter data. IEEE Systems Journal, 16(3), 3554-3565.

[32] Cavraro, G., Comden, J., Dall'Anese, E., & Bernstein, A. (2022). Real-time distribution system state estimation with asynchronous measurements. IEEE Transactions on Smart Grid, 13(5), 3813-3822.

[33] Chen, L., Liu, L., Peng, Y., Chen, W., Huang, H., Wu, T., & Xu, X. (2020). Distribution network operational risk assessment and early warning considering multi-risk factors. IET Generation, Transmission & Distribution, 14(16), 3139-3149.

[34] GU, Y. Z., WU, Z. R., ZHAO, J. G., HAN, L. Q., YUAN, L. L., & HUANG, W. T. (2020, November). Research on intelligent early warning algorithm for distribution network considering extreme climate conditions. In 2020 15th IEEE Conference on Industrial Electronics and Applications (ICIEA) (pp. 412-417). IEEE.

[35] Gu, C., Wang, Y., Wang, W., & Gao, Y. (2023). Research on Load State Sensing and Early Warning Method of Distribution Network under High Penetration Distributed Generation Access. Energies, 16(7), 3093.

[36] Zhou, S., Mao, G., Wen, W., Deng, M., & Guo, M. (2024, October). Digital Twin Early Warning of Operational Risks in Urban Underground Distribution Networks Considering Load Characteristics. In 2024 3rd International Conference on Smart Grids and Energy Systems (SGES) (pp. 56-61). IEEE.

[37] Zhang, K., Dou, X., Li, Y., Bu, Q., Lv, P., Dai, R., & Yu, J. (2024, June). Risk Early Warning and Regulation of Active Distribution Network Based on Imitation Learning. In Frontier Academic Forum of Electrical Engineering (pp. 481-488). Singapore: Springer Nature Singapore.

[38] Gan, J., Ma, H., Sun, F., Fang, M., & Chen, G. (2025, March). Construction and Optimization of Early Warning System for Frequent Blackouts in Active Distribution Network Based on Machine Learning Algorithm. In 2025 International Conference on Electrical Drives, Power Electronics & Engineering (EDPEE) (pp. 799-803). IEEE.

[39] Zhang, H., Wu, Y., Zhang, W., Xu, K., Geng, L., & Yang, H. (2025, March). Online monitoring and early warning of arc grounding fault overvoltage in 10kV distribution system based on Internet of Things technology. In International Conference on Physics, Photonics, and Optical Engineering (ICPPOE 2024) (Vol. 13552, pp. 406-412). SPIE.

[40] Malik, A., & Om, H. (2017). Cloud computing and internet of things integration: Architecture, applications, issues, and challenges. In Sustainable cloud and energy services: Principles and practice (pp. 1-24). Cham: Springer International Publishing.

[41] Ai, Y., Peng, M., & Zhang, K. (2018). Edge computing technologies for Internet of Things: a primer. Digital Communications and Networks, 4(2), 77-86.

[42] Bablu, T. A., & Rashid, M. T. (2025). Edge computing and its impact on real-time data processing for IoT-driven applications. Journal of advanced computing systems, 5(1), 26-43.

[43] Pegoraro, P. A., Meloni, A., Atzori, L., Castello, P., & Sulis, S. (2017). PMU-based distribution system state estimation with adaptive accuracy exploiting local decision metrics and IoT paradigm. IEEE Transactions on Instrumentation and Measurement, 66(4), 704-714.

[44] He, J., Cai, B., Yan, W., Zhang, B., & Zhang, R. (2022). Internet of things-based risk warning system for distribution grid operation state. Journal of Interconnection Networks, 22(03), 2145007.

[45] Huang, Y., Chen, J., Zheng, X., Xie, W., Wang, H., Xie, Z., & Li, Y. (2025). Distribution Network External Force Damage Warning System under Cloud-Edge Collaborative Architecture. Journal of Networking Technology Volume, 16(2).

[46] Netsanet Solomon,Zheng Dehua,Wei Zhang & Teshager Girmaw. (2022). Cognitive Edge Computing–Based Fault Detection and Location Strategy for Active Distribution Networks. Frontiers in Energy Research,10.

[47] Ali Ramyar,Ali Soltani,Mohammad Ramyar & Hamed Najafi Kashkooli. (2025). Urban land use allocation with hybrid linear programming – multi-objective ant colony algorithm. Earth Science Informatics,18(2),415-415.

[48] Keshavarzian Ali, Lahooti Eshkevari Alireza, Abdoli Iman, Karimi Hajiabadi Mostafa, Farzi Mohammad & Arefian Mansour. (2022). A novel bidirectional synchronized transfer method for multilevel electric drive systems based on discrete Fourier transformation. IET Power Electronics,15(11),1034-1046.